Urban Studies and Public Administration
Vol. 4, No. 4, 2021
www.scholink.org/ojs/index.php/uspa
ISSN 2576-1986 (Print) ISSN 2576-1994 (Online)

Original Paper

Analysis of Urban Surface Temperature Using Remote Sensing and Geographic Information System (GIS)

Bernard Tarza Tyubee[1*]& Raymond Nlemadim Chima Anyadike[2]

[1]Department of Geography, Benue State University, Makurdi, Nigeria

[2]Department of Geography, University of Nigeria, Nsukka, Nigeria

[*] Bernard Tarza Tyubee, Department of Geography, Benue State University, Makurdi, Nigeria

Received: October 21, 2021 Accepted: November 8, 2021 Online Published: November 25, 2021

doi:10.22158/uspa.v4n4p16 URL: http://dx.doi.org/10.22158/uspa.v4n4p16

Abstract

The study analysed variation in surface temperature (ST) in Makurdi Urban Area (MUA), Northcentral Nigeria. A total of 12 Landsat TM/ETM+ images were acquired in January, April and June of 1991, 1996, 2001 and 2006. The ST was estimated from the 12 Landsat TM/ETM+ images, grouped into seven classes, and the area of each ST class was determined using remote sensing and Geographic Information System (GIS). The ST magnitudes vary spatially from 27.5^{o}C (water bodies) to 50.7^{o}C (built-up land), representing an intensity of 23.2^{o}C. The mean seasonal ST varies from 32.4^{o}C-34.5^{o}C (cool-dry season), 35.5^{o}C-38.8^{o}C (hot-dry season) and 30.8^{o}C-31.4^{o}C (hot-wet season). The mean annual ST has increased from 32.9^{o}C (1991) to 35.9^{o}C (2006) with ST intensity of 3.0^{o}C. The ST classes of 27^{o}C-29^{o}C and 33^{o}C-37^{o}C recorded the highest loss and gain in area of -126.5km^2 and 94.5km^2 whereas ST classes of 29^{o}C-33^{o}C and 41^{o}C-45^{o}C recorded the least and highest per centage change in area of 22% and 768%. The result showed decreasing and increasing trends in the areas of cooler and warmer surfaces, which are attributed to increase in anthropogen surface materials, with higher heat storage capacities, due to urbanisation.

Keywords

urbanisation, surface temperature, landsat images, remote sensing, geographic information system

1. Introduction

Surface temperature, also refered to as brightness temperature (Chen et al., 2006), is the temperature of radiatively active natural and anthropogenic surface materials that absorb and store radiant energy. Surface temperature (ST), often refered to as land surface semperature (LST), is one of the key parameters controlling the physical, chemical and biological processes of the earth (Pu et al., 2006). The ST or LST forms an important climate variable that related to climate change (Kayet et al., 2016).Surface temperature is important in urban studies because it has considerable impact on urban thermal environment causing urban heat isalnds (UHIs) (Dissanayake et al., 2019) and controls surface heat and water exchange with the atmosphere (Gallo et al., 1993).

Most studies in literature have attributed ST and air temperature patterns in urban areas to changes in surface energy balance. Due to the decrease in vegetation cover and increase in concretised surfaces in most cities, more incoming radiation is converted into sensible heat flux (Q_H) rather than latent heat flux (Q_E) (i.e., higher Bowen ration) resulting to higher surface and air temperature in cities relative non-urbanised areas (Wong & Yu, 2005). Tapper et al. (1981) reported that in rural areas in Christchurch, New Zealand, 40% of the net radiation is used in evaporation (Q_E), 26% goes into sensible heat (Q_H) and 33% into storage (Q_G). By contrast, in the industrial/commercial area, no energy is used for evaporation (Q_E), 64% is converted to sensible heat (Q_H), and 36% goes into storage (ΔQ_S).

Remote sensing is a global application methodology for assessing thermal effect of cities even in regions where pairs of urban and rural temperature records are not available (Gallo et al., 1993). Remote sensing, in conjunction with Geographic Information System (GIS), has been widely applied in detecting land use/land cover change, the basis for the inadvertent climatic modification of cities (Weng, 2001), assessing the distribution characteristics of surface temperature and surface urban heat island (SUHI) (Weng, 2001; Weng et al., 2006) and investigating the relationship between surface temperature and land use/land cover (Zhang et al., 2004; Chen et al., 2006; Yuan & Bauer, 2007). Urban surface heating and temperature exhibit spatial, seasonal and temporal variability in terms of magnitude, intensity and area coverage. Understanding the variation of these characteristics, in the context of land use/land cover change due to urbanisation, is fundamental in urban heat island mitigation, urban planning and design. The major objectives of the study are to: (1) retrieve and estimate ST (^oC) from Landsat EM/ETM+ Images, (2) categorise ST (^oC) in seven classes and (3) analyse the variation in the magnitude and intensity of ST, and areas of the ST classes.

2. Method

2.1 Study Area

Makurdi Urban Area (MUA) is located between latitudes 7° 35' - 7° 53' N and longitudes 8° 24' - 8° 42 'E in Benue State, Northcentral Nigeria, and covers a land area of 800km^2 (Figure 1). The projected population of the study area in 2020 is 460,000 people based on 3.0% growth rate per annum. The MUA is subdivided into eleven political divisions known as council wards. The council wards that cover the metropolitan area are Mission, Clark/Market, Wadata/Ankpa, North Bank I and Wailomayo. Fiidi, Modern Market and North Bank II constitue the suburban council wards and the rural council wards comprise Bar, Mbalagh and Agan (Figure 1). In MUA, 60%, 30% and 10% of the population live in metropolitan, suburban and rural areas (Tyubee, 2021). Like other tropical wet and dry (Aw) climate regions, the study area experienced three thermal seasons namely cool-dry (November-January), hot-dry (February-April) and hot-wet (May-October). The mean seasonal air temperature is 26°C (cool-dry), 31°C (hot-dry) and 28°C (hot-wet) (Tyubee, 2006). Annual rainfall, ranging from 900 to 1,500mm, dominantly occurs between April and October reaching its peak in September.

2.2 Data Acquisition and Processing

A total of twelve (12) Landsat TM/ETM+ images were acquired for a 15-year period (1991-2006). These comprised Landsat 5 TM images (April 11, 1991; June 16, 1991; January 17, 1991; April 25, 1996; June 11, 1996; January 14, 1996) and Landsat 7 ETM+ images (April 13, 2001; June 21, 2001; January 26, 2001; April 12, 2006; June 30, 2006; January 26, 2006) respectively. All the raw images are geo-referenced to a common Universal Transverse Mercator (UTM) co-ordinate system using a 1:50 000-scaled topographical map of the study area and re-sampled the pixel size of the thermal infrared (TIR) band (band 6) to 30m x 30m. The Landsat TM/ETM+ images of the study area were retrieved from scenes of paths 187-188 and rows 054-055 on cloud free days.

2.3 Retrieval and Classification of ST

The retrieval of ST from Landsat TM/ETM+ images was carried out pixel by pixel. The ST of both Landsat TM and Landsat ETM+ data was retrieved from the Thermal Infrared (TIR) band (band 6) using the procedure of Chen, et al. (2006). The procedure for retrieving ST involved the conversion of the Digital Numbers (DNs) of band 6 to radiation luminance (R_{TM6}). The radiation luminance was then converted to satellite brightness temperature in degrees Kelvin (°K). Since the DNs were not first converted to black body temperature, correction for emissivity (ε) was not necessary.

After the retrieval and estimation of ST from each of the 12 Landsat ET/ETM+ images, the ST was then grouped into seven classes namely 27°C-29°C, 29°C-33°C, 33°C-37°C, 37°C-41°C, 41°C-45°C, 45°C-48°C and 48°C-51°C respectively. This classification was necessary due to the nature of high spatial variability of ST in cities and urban areas and the need to analyse the seasonal and annual variation in areas of ST magnitudes.

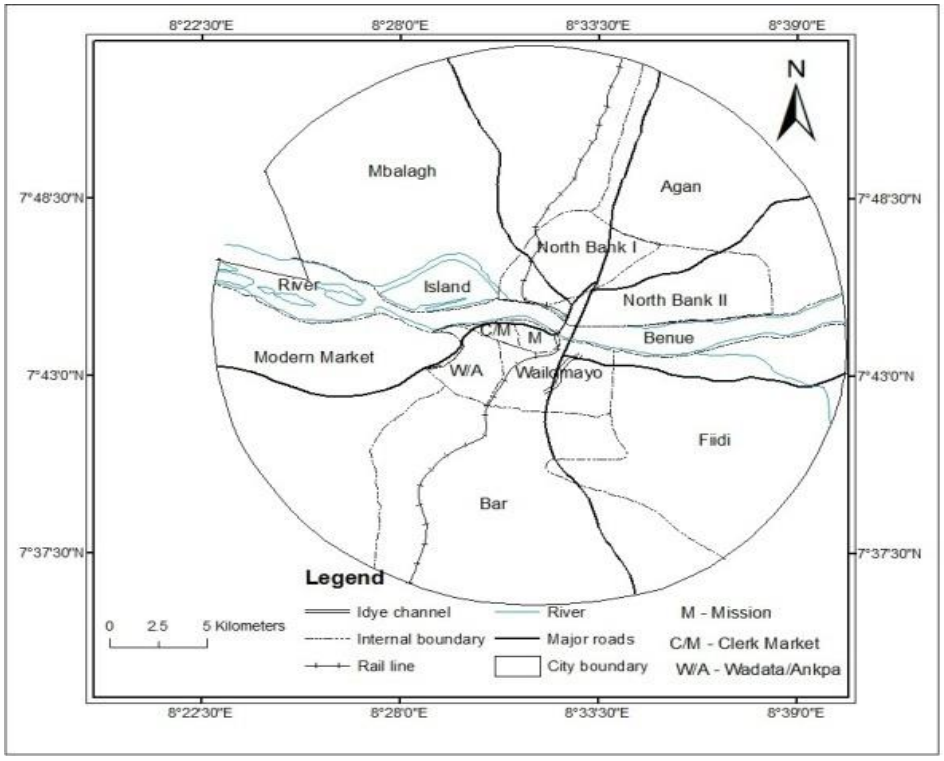

Figure 1. Location and Administrative Units of Makurdi Urban Area

2.4 Data Analysis

The ST magnitudes were estimated pixel by pixel and mapped for each of the 12 Landsat ET/ETM+ images. The seasonal and annual ST magnitudes were computed from the seven ST classes for each of the 12 ST maps using the expression:

$$\frac{\varepsilon fx}{\varepsilon f} \quad (1)$$

Where ε, is summation; x, is the midpoint of each ST class, and f, is the number of pixels for each ST class.

The annual ST magnitudes were then averaged for the three (3) seasons. Standard deviation (σ) was applied to investigate the spatial variation in ST in the study area. The standard deviation was computed for the 12 ST maps from the expression:

$$\sigma = \sqrt{\frac{\varepsilon fx^2}{\varepsilon fx} - \left(\frac{\varepsilon fx}{\varepsilon f}\right)^2} \quad (2)$$

Where ε, x and f remain as in equation 1.

The retrieval, estimation and classification of ST from the 12 Landsat TM/ETM+ images were carried out using ERDAS Imagine 8.6 and ArcGIS 9.2 software.

3. Result

3.1 Variation in ST Magnitude and Intensity

The magnitude and intensity are prominent characteristics of ST distribution. The magnitude refers to the absolute values of ST, whereas the intensity connotes the difference between maximum and minimum ST. The result of spatial, seaonal and annual variation of surface temperature is presented in Tables 1 and 2, and Figures 2-5. The spatial distribution of ST showed that maximum ST was 47.8°C (January), 50.7°C (April) and 47.8°C (June). However, the minimum ST was consistently 27.5°C in all the three seasons and years. This suggests that the ST intensity varied seasonally from 20.3°C (June) to 23.2°C (April). The minimum ST was observed in water bodies and maximum ST occurred in built-up area (Figures 2-5).

Seasonally, the mean ST of cool-dry season (January) showed an increase in ST from 32.4°C (1991) to 34.5°C (2006), with a long term mean surface temperature of 33.5°C and mean intensity of 2.1°C. However, standard deviation showed lower values ranging from 2.6-2.9. In the hot-dry season (April), the mean ST showed an increase from 35.5°C (1991) to 38.6°C (2006), with overall seasonal mean ST of 37.0°C and heating intensity of 3.1°C. The standard deviation for hot-dry season (April) ranges from 2.7 in 2001 to 3.1 in 1996 (Table 2). The ST in hot-wet season (June) ranges from 30.8°C in 1991 to 32.1°C in 2006, with seasonal mean ST of 31.5°C and mean intensity of 1.3°C. The standard deviation however showed relatively lower values, compared to other seasons, ranging from 2.1-2.7 (Table 2). The result indicated an increase in mean ST, in all the three seasons from 1991 to 2006, and the intra-seasonal variation in ST was least and highest in the hot-wet and hot-dry season.

Table 1. The maximum, minimum and intensity of ST in Makurdi Urban Area, 1991-2006

Year	January			April			June		
	Max. temp.(°C)	Min. temp. (°C)	Intensity (°C)	Max. temp.(°C)	Min. temp. (°C)	Intensity (°C)	Max. temp.(°C)	Min. temp.(°C)	Intensity (°C)
1991	47.8	27.5	20.3	50.7	27.5	23.2	47.8	27.5	20.3
1996	50.7	27.5	23.2	50.7	27.5	23.2	47.8	27.5	20.3
2001	50.7	27.5	23.2	50.7	27.5	23.2	47.8	27.5	20.3
2006	50.7	27.5	23.2	50.7	27.5	23.2	47.8	27.5	20.3

Table 2. Mean Seasonal and Annual ST in Makurdi Urban Area, 1991-2006

Year	Cool-dry season		Hot-dry season		Hot-wet season		Annual mean	Annual intensity
	Mean temp. (°C)	STD	Mean temp.(°C)	STD	Mean temp.(°C)	STD		
1991	32.4	2.9	35.5	3.0	30.8	2.6	32.9	4.7
1996	33.2	2.6	36.3	3.1	31.2	2.7	33.9	4.7
2001	34.0	2.9	37.7	2.7	32.7	2.1	35.0	5.1
2006	34.5	2.6	38.6	2.9	32.1	2.2	35.9	5.6
Seasonal Mean	33.5		37.0		31.5		34.0	
Seasonal intensity	2.1		3.1		1.3		3.0	

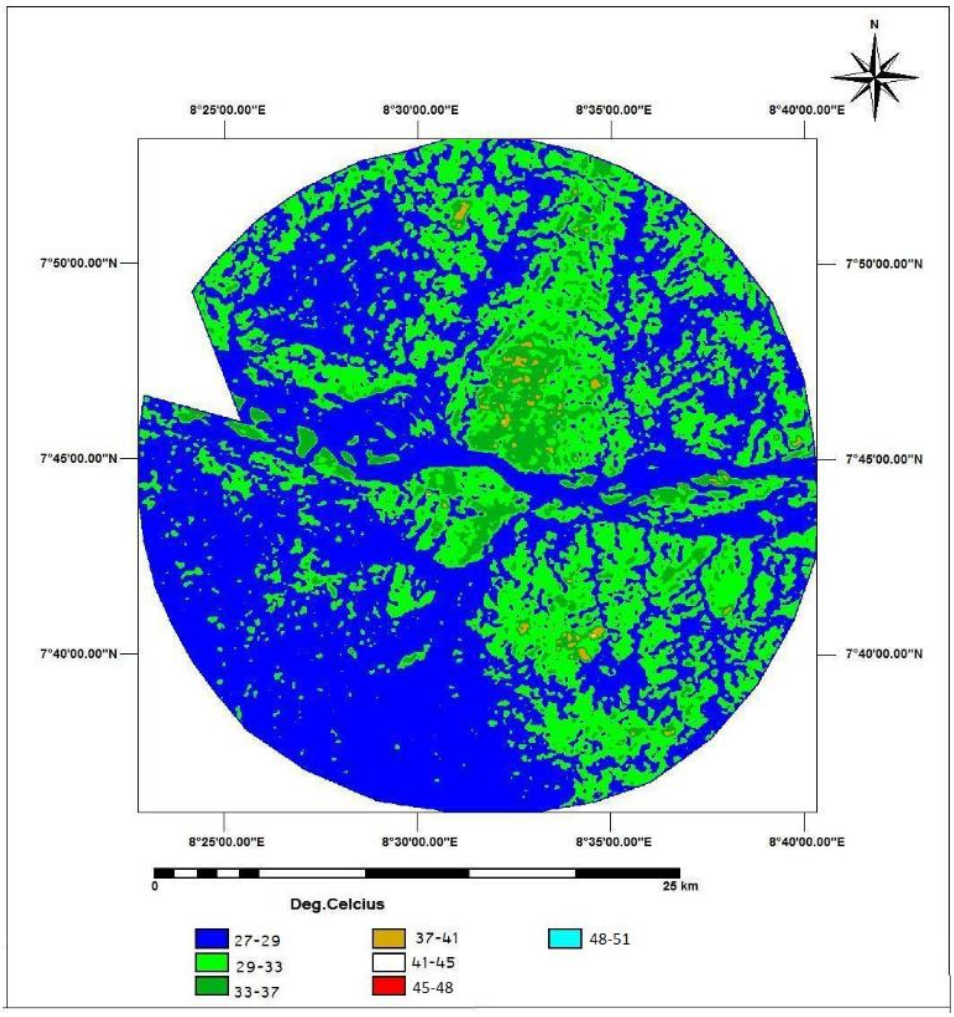

Figure 2. Spatial Distribution of Surface Temperature in Makurdi Urban Area, June 1991

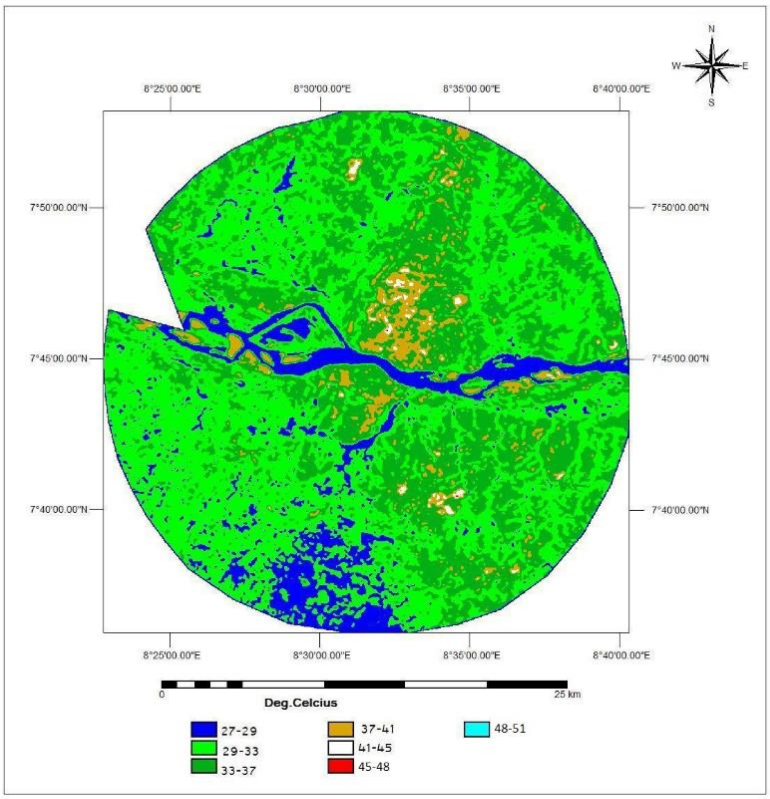

Figure 3. Spatial Distribution of Surface Temperature in Makurdi Urban Area, January 1996

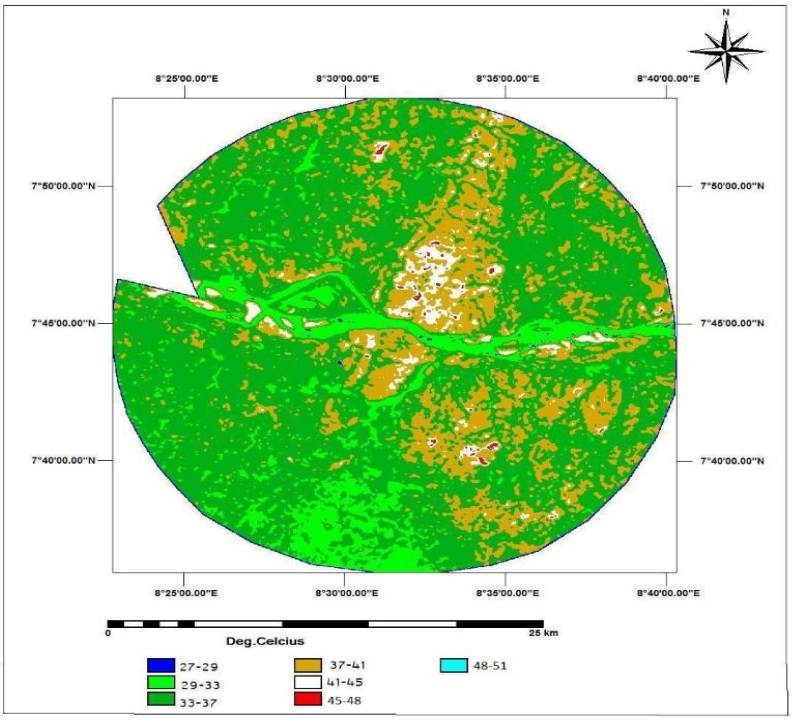

Figure 4. Spatial Distribution of Surface Temperature in Makurdi Urban Area, April 2001

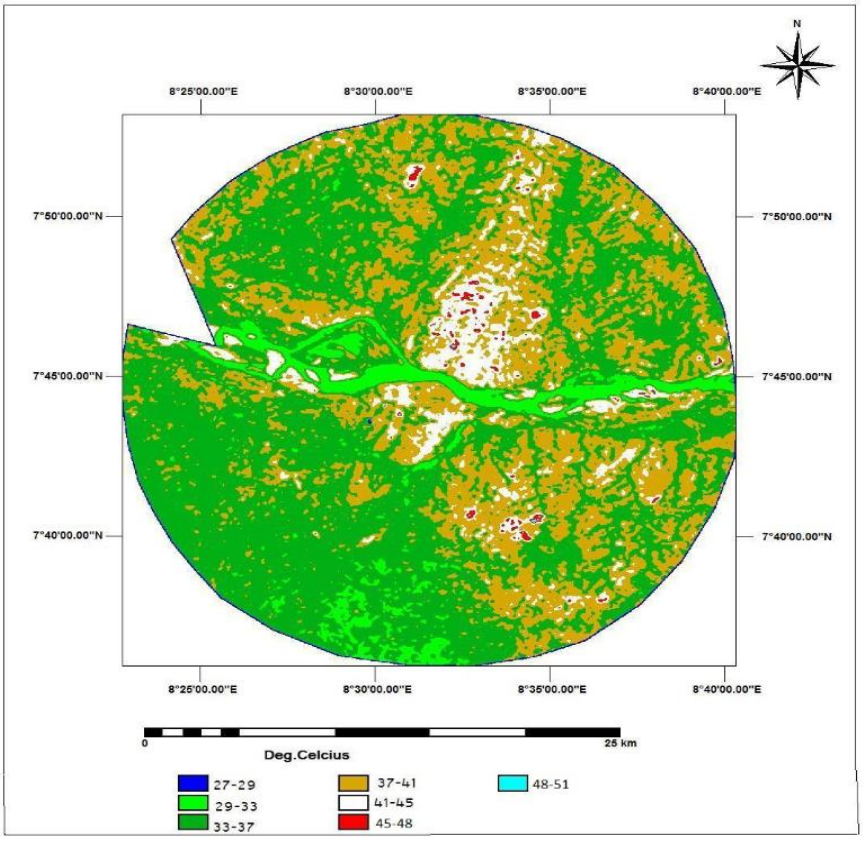

Figure 5. Spatial Distribution of Surface Temperature in Makurdi Urban Area, April 2006

3.2 Variation in Area of ST

The result of the distribution of areas of the seven (7) ST classes is presented in Tables 3-6. The temporal changes in the areas of the seven (7) temperature classes in January showed that ST classes of 29°C-33°C and 45°C-48°C have the largest and least mean areas of 432.8km^2 (54%) and 0.1km^2 (0%) respectively from 1991-2006. Conversely, the ST classes of 41°C-45°C and 29°C-33°C witnessed the largest and least percentage change in area and annual change rate of +1700% and +113% per year and -2% and -0.2% per year during the 15-year period (Table 3).

The variation in areas of the seven (7) ST classes in April indicated that the ST class of 33°C-37°C has the largest mean area of 422.7km^2, representing 53% of total area, and ST class of 48°C-51°C has the least mean area of 0.3km^2(0%). Similarly, the areas of 27°C-29°C and 29°C-33°C ST classes have decreased by 294km^2 (88%) and 22km^2 (73%) from 1991-2006. Conversely, the areas of 33°C-37°C, 37°C-41°C, 41°C-45°C, 45°C-48°C and 48°C-51°C ST classes have increased in sizes by 81km^2 (23%), 187km^2 (238%), 44km^2 (694), 3km^2 (2900%) and 1.3km^2 (130%) respectively within the same period (Table 4).

Moreover, the areas of ST <33°C and >33°C have decreased and increased in sizes from 1991-2006. While the ST classes of 29°C-33°C and 37°C-41°C recorded the highest loss and gain in areas during the

15-year period, the ST classes of 45ºC-48ºC and 29ºC-33ºC recorded the highest and lowest percentage changes in area of +2900% and -88% and annual change rate of +193% and -6% per year (Table 4).

Table 3. Changes in Area (km^2) of Surface Temperature Classes in January

ST classes	1991	1996	2001	2006	Mean area	%	Change in area	%	Rate of change (%)
27ºC-29ºC	269.0	87.6	47.9	28.7	108.3	14	-240	89	6
29ºC-33ºC	399.0	508.1	434.0	390.2	432.8	54	-9	2	0.2
33ºC-37ºC	119.0	183.1	265.0	293.1	215.1	27	174	147	10
37ºC-41ºC	12.6	21.8	50.0	80.3	41.2	5	68	537	36
41ºC-45ºC	0.4	1.4	3.1	7.2	3	0	7	1700	113
45ºC-48ºC	*	*	*	0.5	0.1	0	0.5	50	3
48ºC-51ºC	0	*	*	*	0	0	0	0	0

*Area<0.1km^2

Table 4. Changes in Area (km^2) of Surface Temperature Classes in April

ST classes	1991	1996	2001	2006	Mean area	%	Change in area	%	Rate of change (%)
27ºC-29ºC	30.0	18.8	8.6	8.0	16.4	2	- 22	73	5
29ºC-33ºC	333.8	250.0	79.0	40.0	175.7	22	- 294	88	6
33ºC-37ºC	351.5	399.5	507.2	432.7	422.7	53	81	23	2
37ºC-41ºC	78.3	118.7	182.0	265.0	161.0	20	187	238	16
41ºC-45ºC	6.3	12.6	21.8	50.0	22.7	3	44	694	46
45ºC-48ºC	0.1	0.4	1.4	3.0	1.2	0	3	2900	193
48ºC-51ºC	*	*	*	1.3	0.3	0	1.3	130	9

*****Area<0.1km^2

In June, ST class of 27°C-29°C dominated surface temperature distribution with the highest area of 419.9km^2, representing 52% of total area, followed by ST class of 29°C-33°C (311.1km^2 or 39%), 33°C-37°C (63.7km^2 or 8%) and least by ST class of 37°C-41°C (4.8km^2 or 1%). Moreover, only the area of 27°C-29°C class has declined in size by 116km^2 (24%) from 479.9km^2 in 1991 to 363.5km^2 in 2006. The ST classes of 29°C-33°C and 41°C-45°C have the highest and least gain in areas by 87km^2 and 0.1km^2 respectively. In term of percentage change in area and annual change rate, the ST classes of 37°C-41°C and 27°C-29°C recorded the highest and least percentage change of +103% and +7% per year and -24% and -2% per year (Table 5). The changes in areas of the seven ST classes, Table 6, showed that the largest and least mean areas of 306.4km^2 (38%) and 0.1km^2(0%) belonged to ST classes of 29°C-33°C and 48°C-51°C. However, both ST classes of 27°C-29°C and 29°C-33°C have lost 126.5km^2 (49%) and 72.3km^2 (22%) from 1991-2006, whereas the maximum and minimum gain in area of 94.5km^2 and 0.4km^2 was recorded by ST classes of 33°C-37°C and 48°C-51°C during the period of study. Moreover, during the same period, the ST classes of 41°C-45°C and 29°C-33°C have the highest and least percentage change in area and annual change rate of 768% and +51% per year and 22% and -2% per year respectively (Table 6).

Table 5. Changes in Area (km^2) of Surface Temperature Classes in June

ST	1991	1996	2001	2006	Mean area	%	Change in area	%	Rate of change (%)
27°C – 29°C	479.9	433.0	403.0	363.5	419.9	52	-116	24	2
29°C – 33°C	267.0	302.1	321.2	354.1	311.1	39	87	33	2
33°C – 37°C	50.0	60.7	70.1	78.1	64.7	8	28	56	4
37°C – 41°C	3.1	4.2	5.7	6.3	4.8	1	3	103	7
41°C – 45°C	*	*	*	0.1	0	0	0.1	10	1
45°C – 48°C	*	*	*	*	0	0	0	0	0
48°C – 51°C	0	0	0	0	0	0	0	0	0

*****Area<0.1km^2

Table 6. Annual Variation in Area (km^2) of ST in MakurdiUrban Area from 1991-2006

ST classes	1991	1996	2001	2006	Mean	%	Change in area	%	Rate of Change (%)
27°C-29°C	259.6	119.5	153.0	133.1	181.3	23	-126.5	49	3
29°C-33°C	333.3	353.1	278.0	261.0	306.4	38	-72.3	22	2
33°C-37°C	173.5	214.4	281.0	268.0	234.2	29	94.5	55	4
37°C-41°C	31.3	48.2	79.2	117.2	69.0	9	85.9	274	18
41°C-45°C	2.2	4.7	8.3	19.1	8.6	1	16.9	768	51
45°C-48°C	0	0.1	0.5	1.2	0.5	0	1.2	120	8
48°C-51°C	0	0	0	0.4	0.1	0	0.4	40	3

4. Discussion

The location of the maximum ST or hot spot of 50.7°C, in both south and north bank areas of MUA, coincided with the built-up areas with dense buildings and other human structures. Moreover, the lowest surface temperature (cool spot) of 27.5°C was consistent with River Benue in all the seasons and years emphasising the effect of water surfaces on heat and temperature.

The result of seasonal changes in area surface temperature has revealed that hot-dry season (April) has the highest mean surface temperature and intensity of 37.0°C and 3.1°C, followed by cool-dry season (January) (33.5°C and 2.1°C) and least by hot-wet season (June) (31.5°C and 1.3°C). Moreover, there is higher variability in the distribution of surface temperature in April followed by January and least in June. The result of seasonal variation in magnitude and intensity of ST confirmed Jin (2004) and Yuan and Bauer (2007) findings.

The spatial pattern and seasonal distribution of ST conformed with the observed patterns of land use/land cover changes in the study area (Tyubee, 2021) and were related to seasonal variation in cloud cover, surface and soil moisture, and vegetation cover which affect surface's solar radiation receipt, absorption and storage capacity. It has been reported that the highest and lowest solar radiation in the study area occurred in April and June respectively (Ojo, 1977). In June, cloud cover, humidity and abundant vegetation cover attenuated incoming solar radiation and also converted surface heat into latent heat through evapotranspiration (Weng, Lu, & Liang, 2006). The drier condition and clear skies in April encouraged high solar radiation receipt and absorption by anthropogenic surface fabrics leading to high surface irradiance and consequently high surface temperature.

The result of variation in areas of ST classes showed that ST classes >33ºC have significantly increased in sizes from 1991-2006 while areas of the classes <33ºC have remarkably declined in sizes during the same period. This may be attributed to land use/land cover changes brought by increasing demand for land for socioeconomic activities and infrastructural development at the expense of agricultural land, vegetation cover, wet lands and water resources. Anthropogenic and built-up surface materials are noted for high heat absorption and storage capacity (Bornstein, 1968; McPherson, 1994; King & Grimmond, 1997; Mills, 2004) which result in higher ST.

5. Conclusion

The result of the study revealed maximum and minimum ST of 50.7ºC and 27.5ºC, and ST intensity of 23.3ºC. The maximum mean seasonal ST occurred in hot-dry seasonl, followed by cool-dry season and least in hot-wet season reflecting the seasonal variation in surface receipt of solar radiation and surface heat storage. The annual changes in ST from 1991 to 2006 indicated a general increase in ST from 32.9ºC (1991) to 35.9ºC (2006). The highest ST in 2006 is attributed to the dominance of urban surface materials over natural cover materials, compared to the previous years. The concluded that more warm surfaces have emerged, relative to the cooler ones, during the study period, and the spatial distribution of areas of warmer and cooler surfaces followed the spatial pattern of urbanisation in the study area.

Ackwoledgement

We appreciate the support of management and staff of National Center for Remote Sensing, Jos, Nigeria in acquisition and analysis of Landsat images. The study was partially supported by Doctoral Fellowship of the African Climate Change Fellowship Program (ACCFP) Round 1. The support of the ACCFP Round 1 sponsors and supervisors is also sincerely appreciated. The Late Professor Raymond Nlemadim Chima Anyadike contributed from the conceptualisation to writing of original draft and the paper is dedicated to his memory.

References

Bornstein, R. D. (1968). Observation of the urban heat island effects in New York City. *Journal of Applied Meteorology*, *7*, 575-582. https://doi.org/10.1175/1520-0450(1968)007<0575:OOTUHI>2.0.CO;2

Chen, X. L., Zhao, H. M., Li, P., & Yin, Z. Y. (2006). Remote sensing image-based analysis of the relationship between urban heat island and land use/cover changes. *Remote Sensing of Environment*, *104*, 133-146. https://doi.org/10.1016/j.rse.2005.11.016

Dissanayake, D. M. S. L. B., Morimoto, T., Ranagalage, M., & Murayama, Y. (2019). Land use/land-cover changes and their impact on surface urban heat islands: Case study of Kandy City, Sri Lanka. *Climate*, *7*(19), 1-20. https://doi.org/10.3390/cli7080099

Gallo, K. P., McNab, A. L., Karl, T. R., Brown, J. F., Hood, J. J., & Tarpley, J. D. (1993). The use of NOAA AVHRR data for assessment of the urban head island effect. *Journal of Applied Meteorology*, *32*(5), 899-908. https://doi.org/10.1175/1520-0450(1993)032<0899:TUONAD>2.0.CO;2

Grimmond, S. (2007). Urbanization and global environmental change: Local effect of urban warming. *Cities and Global Environmental Change*, 83-88. https://doi.org/10.1111/j.1475-4959.2007.232_3.x

Jin, M. (2004). Analysis of land skin temperature using AVHRR observation. *Bulletin of American Meteorological Society (BAMS)*, 587-600. https://doi.org/10.1175/BAMS-85-4-587

Kayet, N., Pathak, K., Chakrabarty, A., & Sahoo, S. (2016). Special impact of landuse/land cover changes on surface temperature distribution in Saranda Forest, Jharkland. *Modeling Earth Systems and Environment*, *2*(127), 1-10. https://doi.org/10.1007/s40808-016-0159-x

Kings, T., & Grimmond, C. S. B. (1997). Transfer mechanisms over an urban surface for water vpour, sensible heat and momentum. *American Meteological Society 12thSymposiun on Boundary Layers and Turbulence*, Vancouver, Canada, 455-456.

Mcpherson, G. E. (1994). Cooling urban heat island with sustainable landscape (pp. 455-456). In R. H. Platt, R. A. Rowntree, & P. C. Muick (Eds.), *The ecological city: preserving and restoring urban biodiversity*. Amrhest: The University of Massachussets Press.

Mills, G. (2004). *The Urban Canopy heat Island*. IAUC Teaching Resource. Retrieved May 9, 2007, from http://www.urban-climate.org

Ojo, O. (1977). *The Climates of West Africa*. London: Heinemann London.

Pu, R., Gong, P., Michishita, R., & Sasagawa, T. (2006). Assessment of multi-resolution and multi-sensor data for urban surface temperature retrieval. *Remote Sensing of Environment*, *144*, 211-225. https://doi.org/10.1016/j.rse.2005.09.022

Tapper, N. J., Tyson, P. D., Oulens, I. E. & Hastie, W. J. (1981). Modeling the winter urban heat island over Christchurch, New Sealand. *Journal of Applied Meteorology*, *20*, 365-376. https://doi.org/10.1175/1520-0450(1981)020<0365:VKECOH>2.0.CO;2

Tyubee, B. T. (2006). Inflience of extreme climate on communal disputes and violence in Tivland, Benue State (pp. 93-111). In T. T. Gyuse, & O. Ajene (Eds.), *Conflicts in the Benue Valley*. Makurdi: Benue State University.

Tyubee, B. T. (2021). Estimating per capita land use/lan cover change (LULCC) in Makurdi, Northcentral Nigeria. *Urban Studies and Public Administration*, *4*(1), 97-109. https://doi.org/10.22158/uspa.v4n1p97

Weng, Q. (2001). Modeling urban and growth effects on surface run-off with the integration of remote sensing and GIS. *Environmental Management*, *28*(6), 733-748. https://doi.org/10.1007/s002670010258

Weng, Q., Lu, D., & Liang, B. (2006). Urban surface biophysical descriptors and land surface temperature variation. *Photogrammetric Engineering and Remote Sensing*, *72*(11), 1278-1286. https://doi.org/10.14358/PERS.72.11.1275

Wong, N. H., & Yu, C. (2005). Study of green areas and urban heat island in a tropical city. *Habitat International*, *9*(3), 547-558. https://doi.org/10.1016/j.habitatint.2004.04.008

Yuan, F., & Bauer, M. E. (2007). Comparison of impevious surface area and normalized difference vegetable index as indicators of surface urban heat island effects in landset imagery. *Remote Sensing of Environment*, *106*, 375-386. https://doi.org/10.1016/j.rse.2006.09.003

Zhang, X., Friedl, M. A., Schaaf, C. B., Strahler, A. H., & Schneider, A. (2004). The footprint of urban climate on vegetation phonology. *Geophysical Research Letters*, *31*, LI2209. https://doi.org/10.1029/2004GL020137